**LMA observations of Upward Lightning Flashes at the Säntis Tower Initiated by Nearby Lightning Activity**

A. Sunjerga[1], M. Rubinstein[2], A. Mostajabi[1], M. Azadifar[2], N. Pineda[3,4], D. Romero[4], O. Van der Velde[4], J. Montanya[4], Jordi Figueras i Ventura[5], Nikola Besic[5], Jacopo Grazioli[5], Alessandro Hering[5], Urs Germann[5], G. Diendorfer[6], F. Rachidi[1]

[1] Electromagnetic Compatibility Laboratory, Swiss Federal Institute of Technology (EPFL), 1015 Lausanne, Switzerland
[2] University of Applied Sciences of Western Switzerland (HES-SO), 1400 Yverdon-les-Bains, Switzerland
[3] Meteorological Service of Catalonia, Carrer Berlín 38-46, Barcelona 08029, Spain
[4] Lightning Research Group, Technical University of Catalonia, Edifici TR1, Carrer Colom 1, Terrassa 08222, Spain
[5] MeteoSwiss, Locarno, Switzerland
[6] OVE Service GmbH, Dept. ALDIS (Austrian Lightning Detection & Information System), Vienna, Austria

* Corresponding author. E-mail address: antonio.sunjerga@epfl.ch.

Abstract— We present in this paper lightning current measurements, LMA (Lightning Mapping Array) data and fast antenna electric fields associated with upward flashes observed at the Säntis Tower during Summer of 2017. The LMA network consists of six stations that were installed in the vicinity of the tower at distances ranging from 100 m to 11 km from it. Out of 20 LMA recorded flashes here we analyze in detail four flashes that were triggered by preceding activity (the so-called 'other-triggered flashes'). Based on the lightning activity derived from the European Lightning Detection Network (EUCLID) in an area within 30 km from the tower and within a 5-second time window before the start of the upward tower flashes, only one out of 20 flashes were classified as 'other-triggered'(OT). However, the investigations based on the LMA data reveal that 3 more flashes of the 20 analyzed were preceded by nearby activity and should therefore be classified as 'other-triggered' (OT) flashes. We analyze conditions conducive to the OT flashes, such as the charge structure of the clouds, polarity of preceding leaders and level of activity of the storm. It is shown that all four OT flashes occurred during high LMA activity and a predominantly positive lightning storm.

*Index Terms*—: Lightning mapping array, other-triggered, current, electric field, charge structure, inverted, leader polarity, radar

## 1. Introduction

The characteristics of upward lightning discharges based on tall structure measurements (e.g., Gaisberg, Peissenberg, Säntis) have been widely reported in the literature. However, their initiation mechanisms are still under investigation and not well understood. Wang et al. [1] proposed the classification of upward flashes into two categories: self-triggered (ST) and other-triggered (OT), based on the absence or the presence of other lightning activity in the geographical and temporal vicinity of the tower-initiated flash. The number of ST and OT flashes has been shown to vary depending on the geographical area (e.g., [2]). It has also been shown that the rate of ST versus that of OT flashes is correlated, to some extent, to atmospheric conditions [2-4]. Different observation methods have been used to classify flashes into the ST and OT categories, namely based on data from lightning location systems (LLS) [2], electric fields [5], and video observations [6].

OT flashes can be preceded (or triggered) by both cloud-to-cloud (CC) and cloud-to-ground (CG) flashes. CC flashes can occur on both large scales (a few tens of km) and small scales (a few hundreds of meters), while CG channels extend to a few kilometers [7]. Schumann et al. [8], using video observations, proposed different mechanisms conducive to the initiation of upward flashes, all of them associated with horizontally propagating leaders in the clouds over the towers.

A Lightning Mapping Array (LMA) is a 3D discharge location system pioneered by D. E. Proctor [9-11]. The detection is accomplished by measuring the VHF radiation from the discharges, while the location is determined using the measured arrival times of the common signal at each station to calculate the spatial position and emission time of the radiation source. Proctor used 5 stations to study small-scale breakdowns of lightning. Clustering algorithms [12-14] can be used to automatically identify lightning flashes from LMA data.

In June 2017, a 3D LMA network [15,16], consisting of 6 stations belonging to the Lightning Research Group of the Polytechnic University of Catalonia (UPC) was installed around the Säntis Tower in Northeastern Switzerland. The covered range is typically about 60 km in diameter. The Säntis Tower is equipped with a direct current measuring system since May 2010. The LMA was operational during two months, July and August, 2017).

Out of a total of 20 recorded flashes, we analyze in detail in this paper four for which simultaneous measurements of current and LMA sources associated with OT upward flashes from the Säntis Tower were obtained during the 2017 campaign. This paper is an extended version of paper [17].

## 2. Measurement Setup

### 2.1 Lightning Current and Electric Field Measurements

The 124-m tall Säntis Tower, located at 47°14’57’’N and 9°20’32’’E, is by far the most frequently struck structure in Switzerland [18], [19]. The tower has been instrumented since May 2010 using advanced equipment including remote monitoring and control capabilities for accurate measurement of lightning current parameters enabling a high-resolution sampling of lightning currents over long observation windows [18], [20]. Lightning currents are measured using two sets of Rogowski coils and multigap B-dot sensors located at two different heights along the tower. The analog outputs of the sensors installed are relayed to a digitizing system by means of optical fiber links. The system is equipped with GPS and allows over-the-Internet remote maintenance, monitoring, and control. More details on the instrumentation can be found in [18], [20-23]. The lightning current is recorded over a 2.4 s interval with a pre-trigger delay of 960 ms.

The Säntis measurement station includes also an electric field measurement station comprising a flat-plate antenna and an analog integrator with an overall frequency bandwidth of 30 Hz to 2 MHz, located in Herisau at a distance of 14.7 km from the tower [24].

### 2.2 Lightning Mapping Array (LMA)

An LMA network was installed in the Säntis Tower region in June 2017 [25]. The system consists of six stations measuring VHF radiation in the 60-66 MHz band. The locations of the LMA stations were chosen considering several factors, namely:

1) The magnitude of the local noise within the frequency band,
2) the availability of reliable AC power and communication means,
3) the distance to the source (Säntis Tower), and,
4) a good combination of accessibility and security.

The selected locations correspond to mobile base stations belonging to Swisscom and Swisscom Broadcast and they are shown in Fig. 1. The measurement stations were deployed in the vicinity of the Säntis Tower, at distances ranging from 100 m to 11 km. The area of interest is located in eastern Switzerland and it covers parts of the cantons of Appenzell Inner-Rhodes, Appenzell Outer-Rhodes,

and St. Gall. The LMA takes the maximum power of VHF radiation within a time window of 80 microseconds and measures the time of arrival with 50 ns accuracy using a PC-based digitizer card coupled to a GPS receiver.
The LMA data were synchronized with the lightning current data using GPS time stamps. Results from the LMA network were transformed from global coordinates to the local coordinate system of the tower taking into account the curvature of the Earth. The coverage of the LMA system is about 30 km to the west of the tower, about 15km to east and 25 km to south and north (for more details see [17] in Fig. 1.]

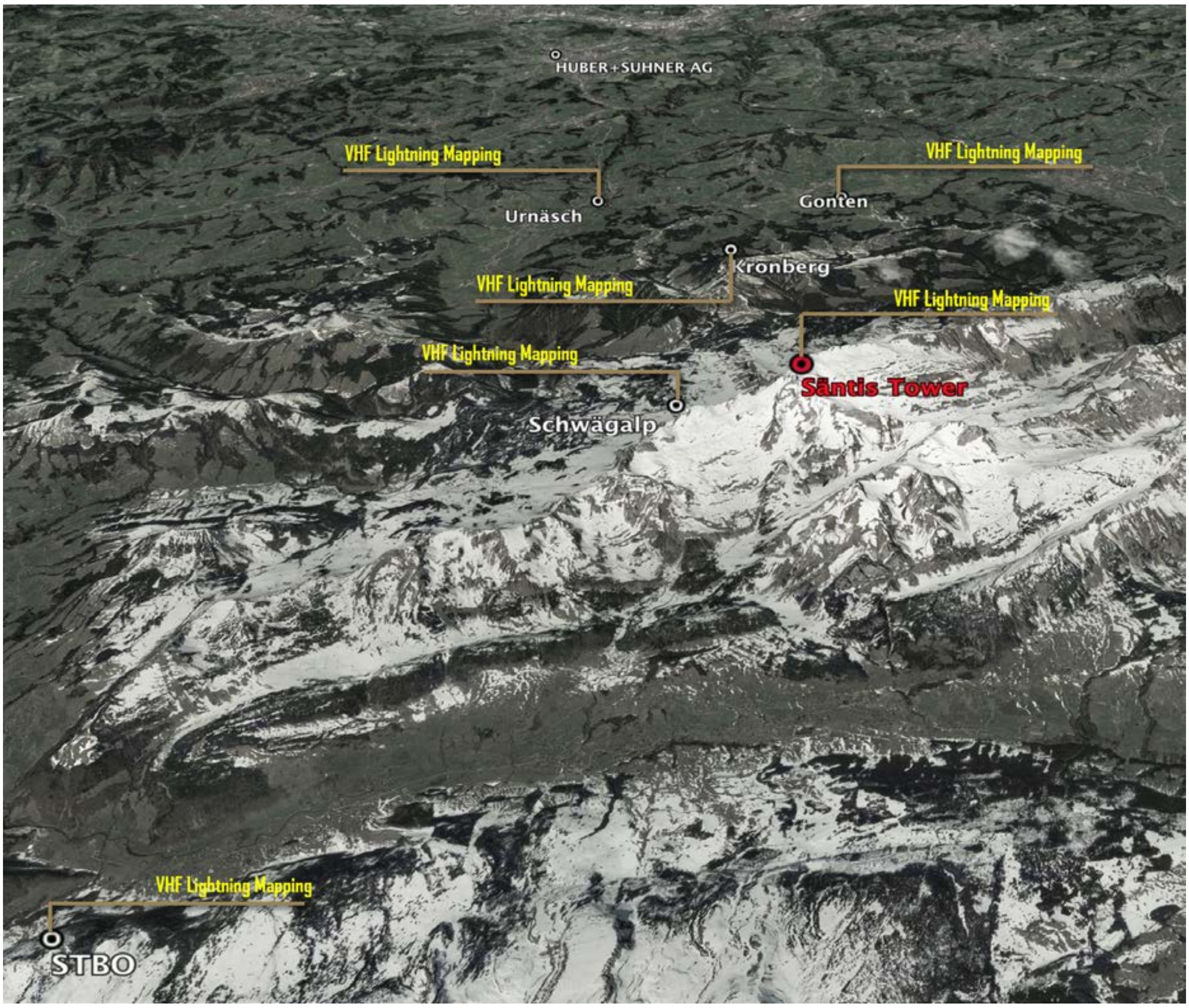


Fig. 1. Lightning mapping array stations around the Säntis Tower. The measurement stations were deployed in the vicinity of the Säntis Tower, at distances ranging from 100 m to 11 km. The electric field station is located 14.7 km north of the tower at the top of Huber+Suhner building shown in the figure.

## 3. Observations of Other-Triggerd Flashes

### 3.1 Overall Data

During the campaign, lightning currents, electric fields and LMA data were simultaneously recorded. In this paper, we present results for 20 analyzed flashes in the period from 29.06.2017 to 18.07.2017. The electric field system was operational only during three of the flashes. Using the data from the EUCLID network [26,27], the flashes were classified either as OT or ST, considering whether or not lightning activity was reported in an area within 30 km from tower and within a 5-s time window before the start of the flash. Using these criteria, all 20 flashes (18 negative, 1 positive and 1 bipolar) were initially classified as ST in [25]. High level of noise in low frequency spectrum of the Rogowski coil lightning measuring system made it hard to determine the exact current onset time at the tower. More detailed analysis with application of a lowpass 1-kHz filter in this paper showed that actually one flash in [25] using EUCLID was misclassified as ST. That upward negative flash was preceded by a downward positive, single-stroke flash recorded about 100 ms before the start of the ICC, about 22 km East and 11 km South of the tower, in an area without LMA coverage. Since the preceding event was not in the area of LMA coverage, the flash from the tower was not classified as OT using the LMA.

On the other hand, using the LMA, we could observe that 3 more flashes were of the OT type. Schumann et al. [2017] observed three different types of preceding flashes from which the upward lightning can be triggered: (i) a return stroke (RS) that leads to an intensification of a horizontal leader over the tower that, in turn, triggers the upward lightning in the tower, (ii) an extension over the tower of the horizontal part of a leader during the continuing current (CC) phase of a nearby CG flash, and (iii) an in-cloud leader that develops over the tower, and whose other end may or may not terminate in the ground. All of the three LMA recorded OT flashes belong to category (iii) and, consequently, are poorly recognized by any lightning location system. It is unclear to which type the OT flash recognized by EUCLID belongs since the LMA did not detect any activity over the tower at the time of initiation of the upward flash. Note that the preceding return stroke is located outside of the coverage areas of the LMA.

In what follows, we will present one positive OT flash and two negative OT flashes that occurred during a period of just 3 minutes. Data for the third negative OT flash classified by EUCLID will not be shown here since the preceding flash was not covered by the LMA. However, the data can be found in the attached materials. The time evolution of LMA sources for each flash can also be observed in the accompanying animations. We will analyze the charge structure of the cloud as well as the polarity of the leaders.

Since the negative leaders propagate through positive charge regions and radiate more strongly (compared to positive leaders) in the VHF spectrum [28], the LMA observations over longer periods can be used to infer the charge structure of the cloud. The average horizontal speed can be used to estimate the polarity of the leader. Van der Velde and Montanyà [29] showed that negative leaders propagate with an average speed of $10^5$ m/s (during positive cloud to ground flashes, the speed can sometimes go up to $10^6$ m/s), while the average speed for positive leaders is around $2x10^4$ m/s. In the following analysis, one has to have in mind the limitation of the LMA. Mazur et al. [2013] argued that the TOA lightning mapping technique does not allow the simultaneous processing of both the strong radiation signals from negative breakdowns and the much weaker radiation signals from positive breakdowns. It is not clear for any of the floating leaders if they occurred in a bidirectional [30] or a unidirectional manner. The LMA also has a low efficiency in detecting leaders such as dart leaders or K changes propagating along already ionized paths.

### 3.2 Negative Flashes

#### 3.2.1 Charge Structure

Two negative other-triggered flashes occurred in a time interval of just below 3 minutes and a third one followed about 22 minutes after the first one. The high VHF activity in the 20-minute period centered at the time of the first other-triggered flash is presented in Figure 2, in which the inferred positive and negative charge regions are shown.

Radar data [31] suggest that the cloud extended to a height of about 12 km and the melting layer can be observed at about 3 km. No charge is expected below the melting layer. The wind speed at the location of the Säntis was 24.1 km/h with an angle of 253°, approximately from West (as shown with the black arrow on the Fig 2b). The temperature at the summit of the Säntis was measured to be 10.7 °C with a relative humidity of 75%. During the considered 20-minute period, the lightning activity was predominantly positive with EUCLID reporting 103 positive strokes and 55 negative strokes. Although the ratio of positive to negative strokes is about 2, the ratio of the numbers of flashes is much higher since positive lightning typically consists of a single return stroke while negative flashes typically have 4-5 strokes. Twenty of the EUCLID-detected negative strokes correspond to return strokes/ICC pulses belonging to the two Other-Triggered events initiated from the tower. In Fig. 2 we infer the charge polarity based on the LMA sources density level. A high number of LMA sources can be observed at altitudes ranging from 4 to 11 km, suggesting that these altitudes correspond to the main positive charge region. It is possible that there exists a shallow negative charge region just below the main positive region characterized by a lower number of LMA sources. This might be due to the corona discharge from the ground. Similarly, the lower number of LMA sources at altitude of about 11 km suggests either a negative charge region or the termination of cloud structure. The charge structure shown in Fig. 2 is inverted from the normal tripole charge structure observed during the thunderstorms with dominant negative lightning flashes. The altitude of the positive charge region is much lower than usually observed during the occurrence of positive flashes. The exact charge structure might be much more complex than one presented in Fig. 2 with possibly different charge polarities at the same altitude.

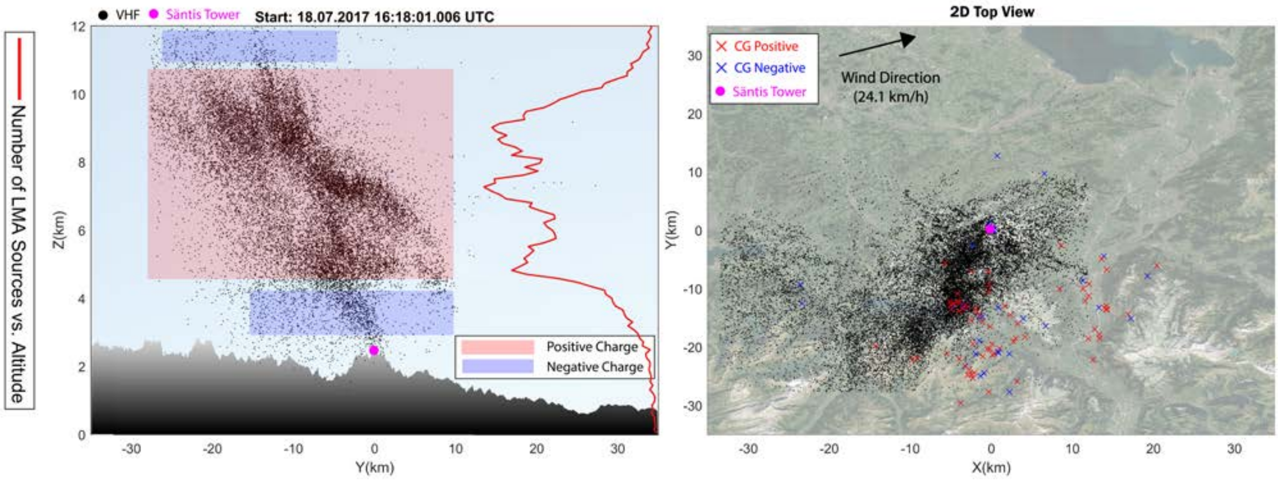


Fig. 2. VHF activity recorded by the LMA stations in the Säntis region over a 20-minute time window starting 10 minutes prior to the initiation of two negative flash to the tower. Left panel: 2D side view with histogram of LMA sources vs. altitude. Right panel: 2D top view. EUCLID recorded flashes are shown with crosses (blue for negative and red for positive). The negative and positive charge regions, inferred from the LMA source density, are shown, respectively, in blue and red. The position of the tower is shown with a purple marker.

### 3.2.2 LMA Observations

Fig. 3 presents the obtained data for the first upward negative OT flash. The start of the initial continuous current (ICC) occurs at about 100 ms as marked with black arrow on Fig. 3c. The flash was preceded by in-cloud discharge activity as can be seen from the LMA data (red arrows marked with number 1). This activity was initiated at different altitudes (from about 2 to 10 km) west of the tower, propagating in different directions, south, north and east towards the tower, and presumably causing an electric field intensification at the tower tip, resulting in the initiation of an upward flash.

Fig. 4 presents the horizontal distance from the tower to the ground-plane projection of the detected LMA sources as a function of time. Blue and black straight lines were drawn in the plot of Fig. 4 with slopes corresponding to the typical positive leader speed ($2 \times 10^4$ m/s) and negative leader speed ($2 \times 10^5$ m/s). By use of speed criteria, we can infer the leader polarity. Due to the relatively low number of detected LMA sources and leader branching, the estimation is somewhat difficult. The trend in the data shown in Fig. 4 is not so clear in the first 80 ms. Beyond this time, there is a clear indication—of the characteristic horizontal speed of negative leader. The presence of the initial continuous current in the tower-base current indicates that the flash was of upward type. From the negative sign of the ICC, we can conclude that the leader was positive. No LMA sources associated with the upward leader are recorded, since they are probably obscured by stronger radiation from the negative leader (shown with orange arrow #2) as discussed by Mazur et al. [2013]. Most of the LMA sources belonging to the negative in-cloud leader are located at an altitude of about 5 km, again suggesting that the positive charge region is at that height, consistent with the observed LMA density of sources in Fig 2.

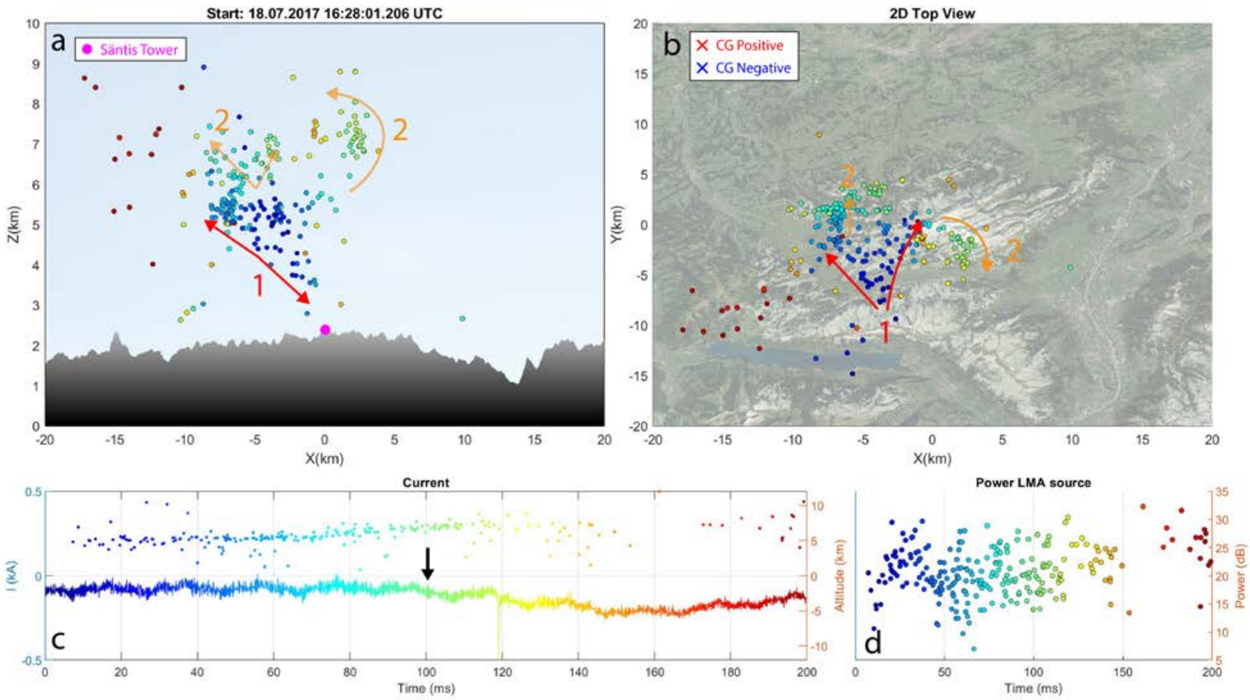


Fig 3. Initial stage of an upward negative flash initiated from the Säntis tower recorded on 18.07.2017 at 16:28:01 UTC. In the plots, the location of the tower is shown with a purple marker and the LMA VHF sources are shown with time-coded circle markers. (a) 2D view of Z vs. X, (b) 2D view of X vs. Y, (c) current with VHF sources superimposed (1 kHz low-pass filter applied), (d) power vs. time for the VHF sources. Note that the colors of arrows are not color-coded for better contrast.

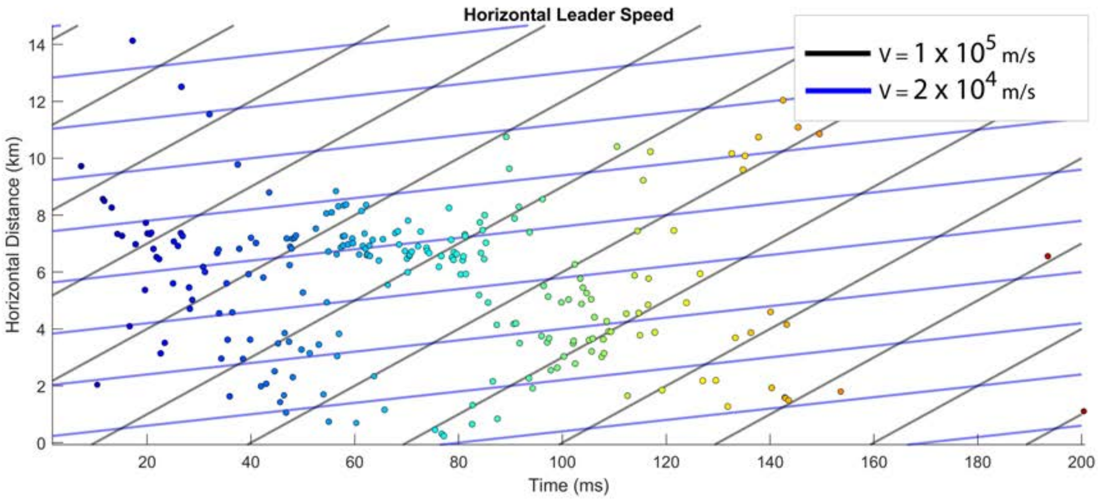


Fig. 4. Horizontal leader speed during the initial stage of the flash. The slopes of the blue and black straight lines correspond to the typical speeds of positive and negative leaders, respectively.

Observations for the complete duration of the flash are shown in Fig. 5. Note that the current in Fig. 5c is now shown in logarithmic scale. As can be seen from Fig. 5b, the length of the in-cloud leader was more than 40 km, covering a surface of about 800 $km^2$. The leader propagated in various directions and it probably obscured the activity of the flash at the tower both during the ICC and during the return stroke (RS) phases. Most of the RSs were detected by EUCLID. The extension of the in-cloud leader continued even after the last RS of the tower flash as can be seen from Fig 5c. The analysis of the leader horizontal velocity (not shown here) suggests negative polarity for the leader during the later stages as well as during the initial stage. Interestingly, a positive CG flash was observed by EUCLID, which has presumably induced the fast current impulse at the tower marked with the black arrow.

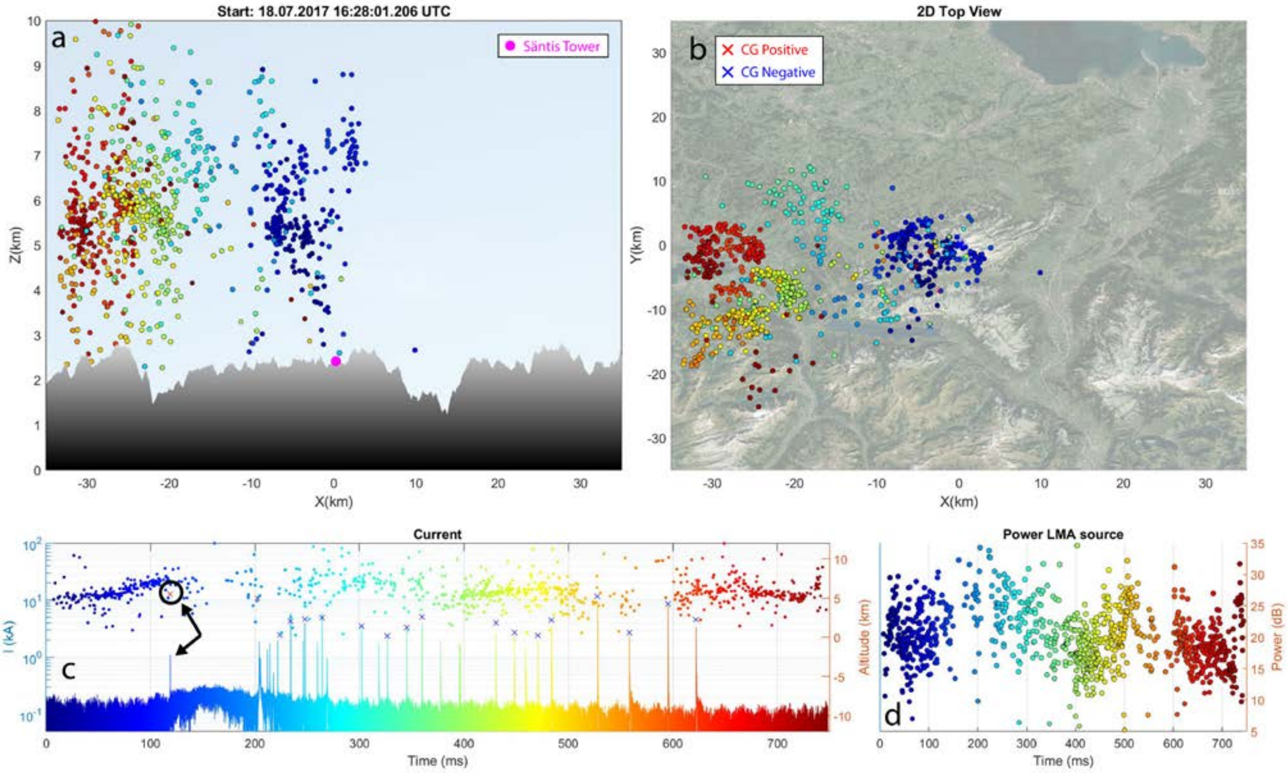


Fig 5. Upward negative flash initiated from the Säntis tower that occured on 18.07.2017 16:28:01 UTC recorded over the flash's whole duration. In the plots, the location of the tower is shown with a purple marker and the LMA VHF sources are shown with time-coded circle markers. (a) 2D view Z vs. X, (b) 2D view of X vs. Y, (c) current magnitude in logarithmic scale with superimposed VHF sources, (d) power vs. time for the VHF sources. Note that the colors of arrows are not color-coded for better contrast.

Observations on the first 350 ms of the second negative OT flash are shown in Figure 6. The ICC current started at about 100 ms. Again, we can conclude from the ICC and current polarity that an upward positive leader from the tower initiated the flash. The LMA sources of the negative (as can be seen in Fig. 7) in-cloud leader started before the onset of the ICC (red arrows #1), at about 25 ms. As in the previous flash, most of the LMA sources from the preceding negative leader were detected at an altitude of 4-7 km, suggesting that the positive charge region was at that altitude, consistent with Fig 2. The upward positive leader was obscured again by strong radiation from a negative in-cloud leader (orange arrow #2). The ICC ended before the onset of first RS and only one LMA source was recorded during the six return strokes.

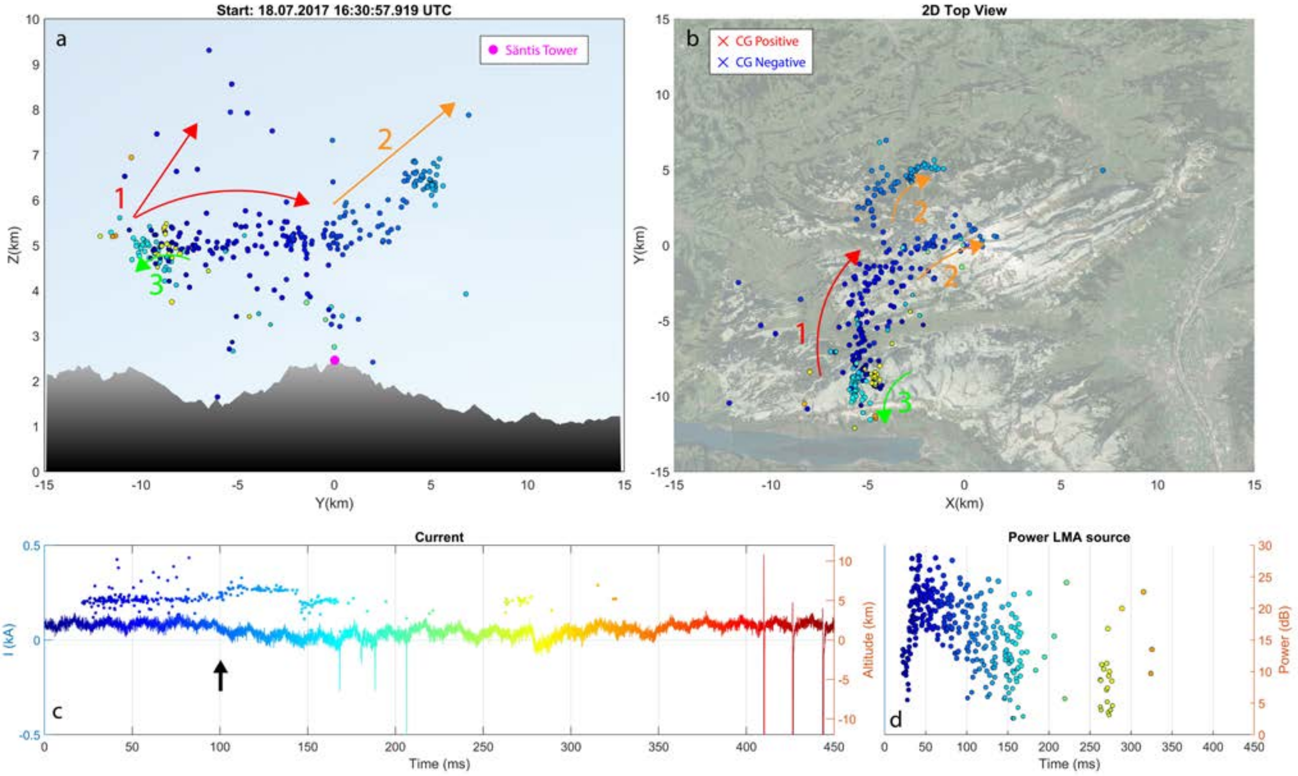


Fig 6. Initial stage of an upward negative flash initiated from the Säntis tower recorded on 18.07.2017 at 16:30:57 UTC. In the plots, the location of the tower is shown with a purple marker and the LMA VHF sources are shown with time-coded circle markers. (a) 2D view Z vs. ~~X,~~ (b) 2D view of X vs. Y, (c) current with superimposed VHF sources (1kHz low pass filter applied), (d) power vs. time for VHF sources. Note that the colors of arrows are not color-coded for better contrast.

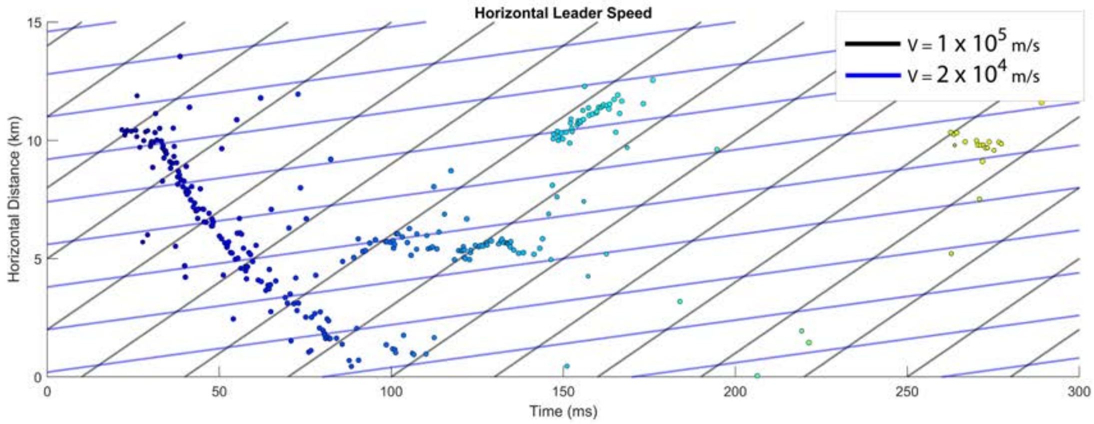


Fig. 7. Horizontal leader speed during the initial stage of the flash

### 3.2.3 Electric Field vs. Current

Fig. 8 and Fig. 9 present the time synchronized waveforms of the electric field measured at 14.7 km from the tower and the current measured at Säntis Tower. In both cases, we can observe the rise of the electric field, caused by the in-cloud leader, prior to the initiation of the current. The delay time of the current is consistent with the delay time from the first LMA sources measured in Fig 3. and Fig. 6. The in-cloud leader propagated during the whole duration of the first negative flash, which can be seen both from the continuous electric field in Fig. 8 and from LMA observations in Fig. 4. In the case of the second flash, the in-cloud leader ceased to exist prior to the return strokes phase, which can be seen in

Fig. 9.

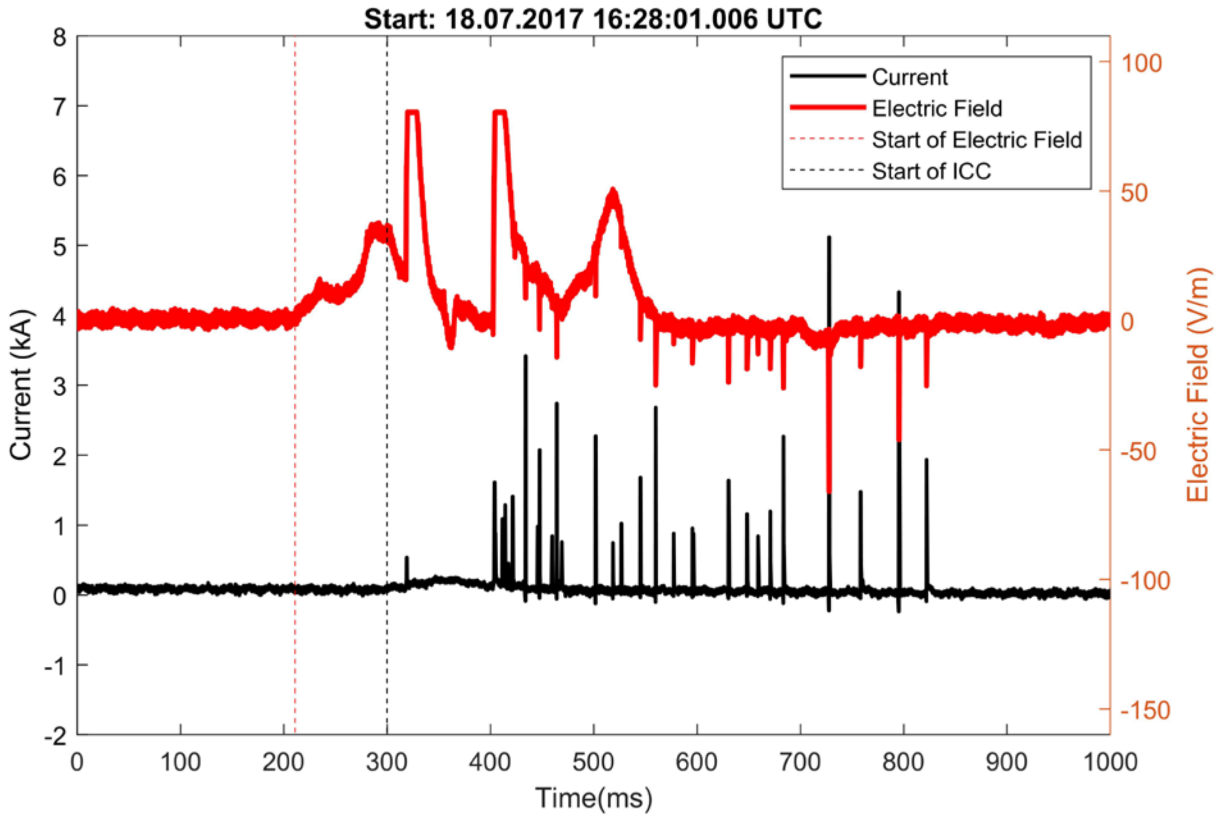


Fig 8. Electric field at 14.7 km vs. current at the tower filtered with a 1-kHz lowpass filter. Recorded on 18.07.2017 at 16:28:01 UTC. Note that the sign off current is negative to emphasize syncronization with electric field.

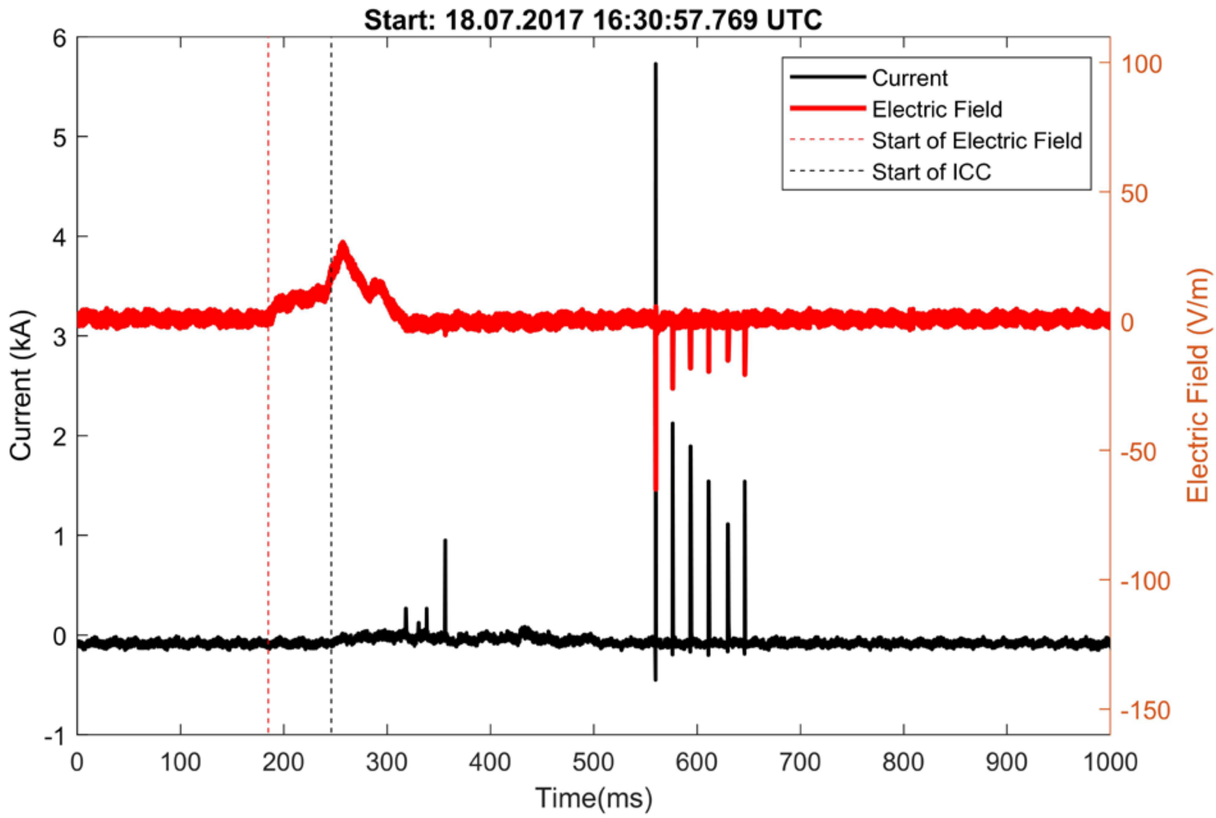


Fig 9. Electric field from the fast antenna vs. the current at the tower filtered with 1-kHz lowpass filter. Recorded on 18.07.2017 at 16:30:57 UTC. Note that the sign off current is negative to emphasize

syncronization with electric field.

### 3.2.4 Skech of Process

Figures 10 and 11 show a simplified sketch of the initial stage of the two observed negative OT flashes. In the case of the first flash (Fig. 10), a leader started West of the tower at an altitude of about 5 km and it propagated in three different directions. Even though the polarity of the leader is not completely clear from the horizontal speed criteria, we have assumed it to be negative. It is possible that upper part of the leader is positive and that in-cloud leader propagated in bidirectional manner with positive end upward and negative downward. This would require the existence of local negative charges at the height of the upper part of the leader (at about 6km). As one end neared the tower, the upward positive leader (in red) was initiated. The fact that the in-cloud leader (the end of the leader propagating away from the tower) continued to extend as a negative leader suggests that the two leaders did not connect. The positive leader was probably triggered by the proximity of the incoming negative leader but it propagated into the shallow negative charge layer below the main positive region.

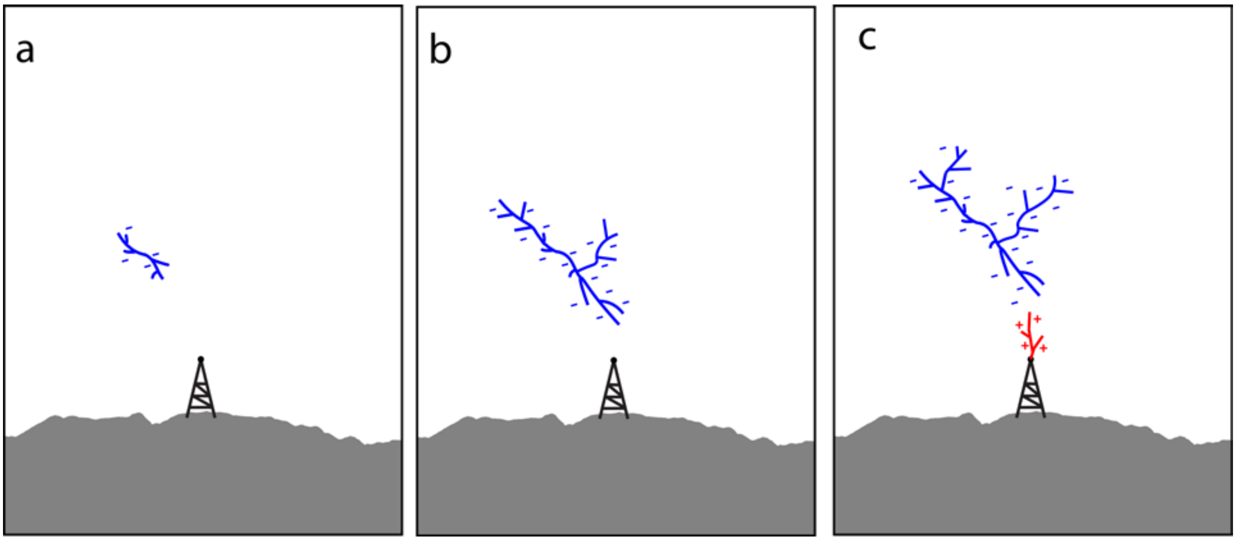

Fig 10. Sketch of the initial phase of the flash initiated from the Säntis tower on 18.07.2017 at 16:28:01 UTC. View from the South. Not to scale.

The second flash started similarly West of the tower and it propagated in two directions, one horizontal above the tower and one propagating both vertically and horizontally. Again, we cannot rule out the existence of positive leader in the opposite direction to the East that was possibly obscured by the strong radiation of negative leaders. As the horizontal portion reached the region above the tower, a positive upward leader was initiated. There are not enough LMA sources to use the horizontal speed criterion to distinguish the polarity of the leaders during the return strokes and to ascertain whether this upward leader connected to the in-cloud leader or not.

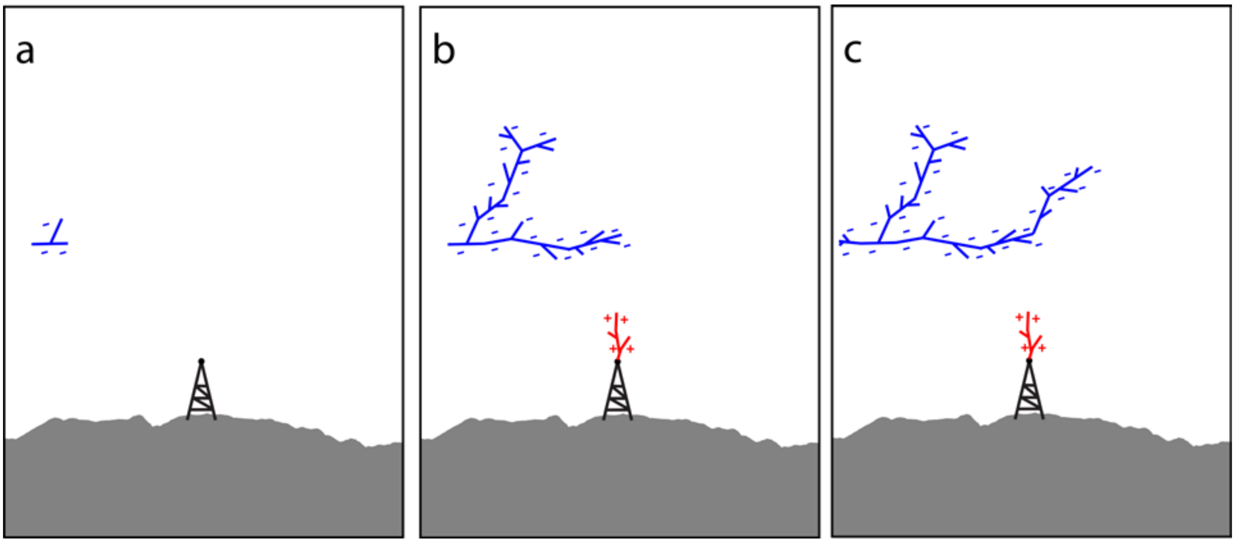

Fig 11. Sketch of initial phase of the flash initiated from the Säntis tower recorded on 18.07.2017 at 16:30:57 UTC. View from the East. Not to scale.

### 3.3 Positive Flash

#### 3.3.1 Charge Structure

The high VHF activity in the 20-minute period centered at the time of the positive OT flash that occurred on 29.06.2017 at 13:28:27 UTC is presented in Figure 12. Radar data [31] suggest that the cloud extended to a height of about 10 km and the melting layer was at about 2.5-3 km. The wind speed at the location of the Säntis was 6.1 km/h with the angle of 186°, approximately from the South (as shown with a black arrow in Fig. 12b). The temperature at the altitude of the Säntis tower was 4.2 °C, with a relative humidity of 100%. Again, during the considered 20-minute period, high activity was recorded by EUCLID, which reported 40 positive strokes and 163 negative strokes. As mentioned earlier, the fact that positive flashes consist generally of a single stroke while negative flashes contain on average 4 to 5 pulses implies a higher number of positive flashes. A high number of LMA sources can be observed at altitudes ranging from 3 to 6 km, suggesting that the main positive charge region was located in that height range as illustrated in Fig. 12. Positive charge layer is closer to the ground, comparing with the charge structure in Fig. 2 we can observe even lower. It is not clear if there exist shallow negative layer bellow. Main negative charge layer is possibly located at altitudes ranging from 6 to 10 km.

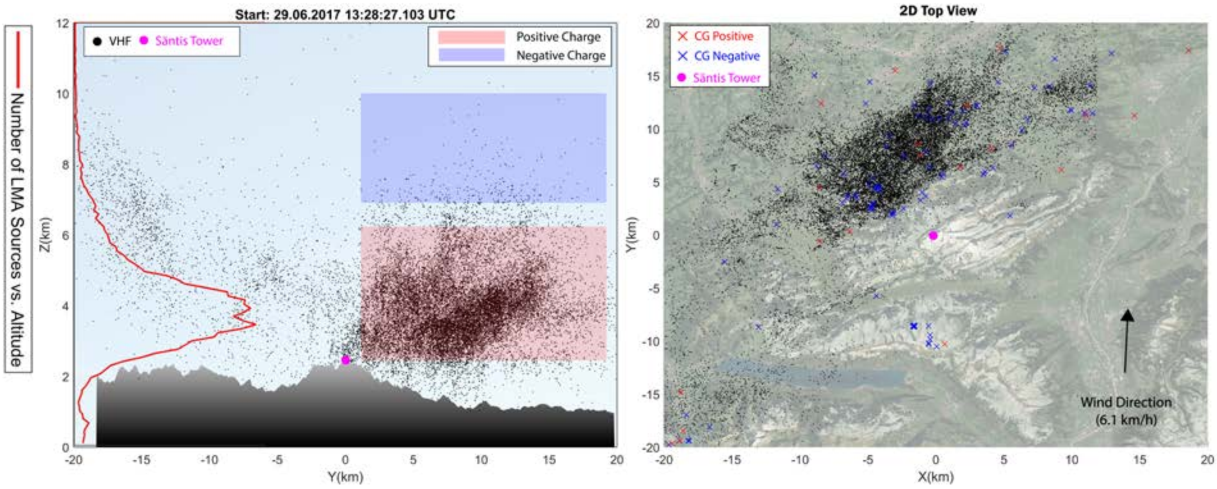

Fig. 12. VHF activity recorded by the LMA stations in the Säntis region over a 20-minute time window starting 10 minutes prior to the initiation of an OT positive flash to the tower (29.06.2017 at 13:28:27 UTC). Left panel: 2D side view with histogram of LMA sources vs. altitude. Right panel: 2D top view.

EUCLID recorded flashes are shown with crosses (blue for negative and red for positive). The negative and positive charge regions, inferred from the LMA source density, are shown, respectively, in blue and red. The position of the tower is shown with a purple marker.

### 3.3.2 LMA Observations

Fig. 13 presents simultaneous measurements of current and LMA sources for the case of the positive flash. The flash is preceded by an in-cloud leader marked with red arrows number #1. This leader propagated vertically to ground and branched horizontally and was classified as negative using the criteria for horizontal velocity. This leader was followed immediately by the upward negative leader from the tower (arrow #2). The polarity of this leader can be inferred from the current waveform. The positive current waveform at the tower lasted for about 6 ms. It should be noted that it is also possible that the flash was actually an aborted leader which never reached the positive cloud charge. This was followed by some LMA activity at the location of the preceding in-cloud flash.

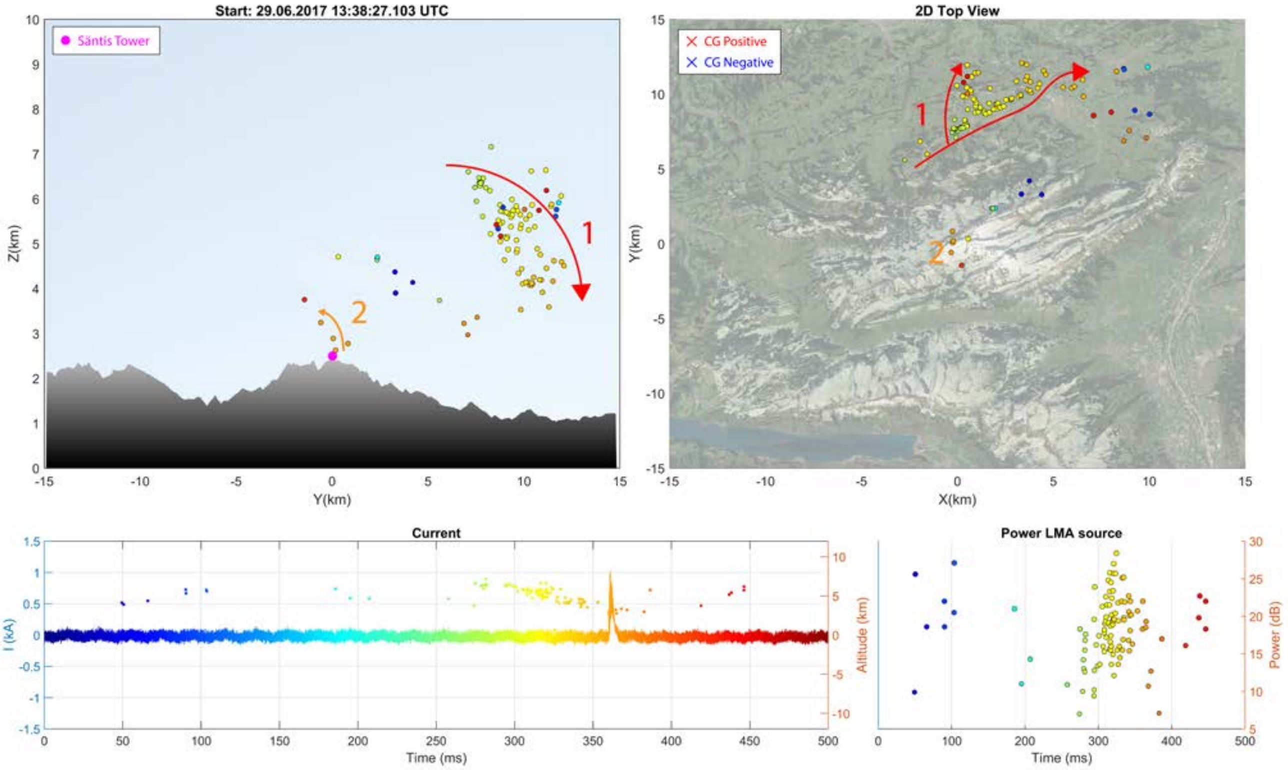


Fig 13. Data associated with the upward positive flash of Fig. 12, with a particularly small peak value of about 1 kA. Again, for this case, the LMA data reveal cloud activity starting from about a second prior to the initiation of the upward positive flash. The activity originated about 7 km north of the tower and it moved towards the East. The in-cloud leader propagation from 5 to 3 km height in the immediate vicinity of the tower can be distinguished by observing the time evolution of the VHF sources. Again, this flash should have been classified as an OT flash. Note that the colors of arrows are not color-coded for better contrast.

### 3.4.3 Skech of Process

Figure 14 presents a simplified 2D sketch of the positive flash described in the previous section. The in-cloud negative leader started North from the tower and propagated verticaly toward the ground. Again, the possibility of a positive leaader propagating upward and obscured by stronger radiating negative leader cannot be ruled out. When the negative leader reached an altitude of about 3 km, another negative leader was initated from the tower. Soon after, that LMA activity vanished.

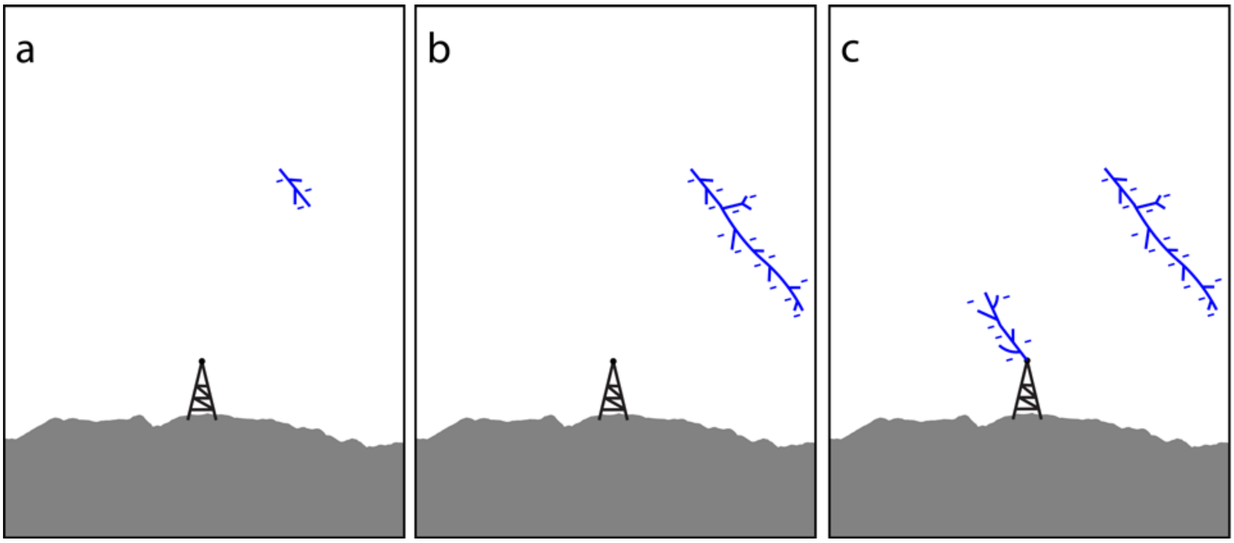


Fig 14. Sketch of the positive flash initiated from the Säntis tower recorded on 29.06.2017 at 13:28:27 UTC. View from the East. Not to scale.

**4. Comparison with Self-Triggerd Flashes**

All three OT flashes occurred during storms with predominantly positive lightning. The preceding events overlap with the triggered flashes. During the 20 minutes centered around the first negative (#18) OT flash, 24’-421 LMA sources were recorded. If we classify any period with no LMA sources in the covered range for 100 ms or more as no-activity during these 20 minutes, the no-activity period amounts to 97.6% of the total time, showing that the random overlapping of events has a probability of 2.4%. For the case of the third negative flash classified as OT by EUCLID, some of the storm activity occurred outside of the LMA coverage range and we observed a lower LMA activity of 0.68 %. The positive OT flash was characterized with LMA activity of 3.95%. The average LMA activity corresponding to the four OT flashes in the observed period is 2.35 %.

Twelve out of 16 ST flashes occurred during periods without any positive flash within the 20-minute period centered at the time of the flash. All of the ST flashes occurred during storm with dominant negative lightning flashes. ST flashes occurred during less active thunderstorms. LMA activity ranged from 0.01 to 1.67% with an average value of 0.35%, almost seven times lower than in the case of OT flashes. Interestingly, two flashes (#5 and #7) occurred without any LMA activity 10 minutes prior to the flash. The summary activity of the 20 analyzed flashes is shown in Table 1.

| Table 1. Percentage of LMA active period (period with no more than 100 ms without LMA sources) | | | | | | | | | | |
|---|---|---|---|---|---|---|---|---|---|---|
| Flash number | 1 | 2 | 3 | 4 | 5 | 6 | 7 | 8 | 9 | 10 |
| Date | 29.06.17 | 29.06.17 | 29.06.17 | 29.06.17 | 29.06.17 | 29.06.17 | 29.06.17 | 29.06.17 | 29.06.17 | 29.06.17 |
| UTC Time | 13:38:27 | 14:06:13 | 14:08:39 | 14:11:09 | 15:05:42 | 15:10:52 | 15:36:50 | 15:39:46 | 15:45:52 | 15:47:31 |
| Polarity | P | N | N | N | N | N | N | N | N | N |
| Type | OT | ST | ST | ST | ST | ST | ST | ST | ST | ST |
| LMA Active (%) | 3.95 | 1.67 | 1.15 | 0.83 | 0.04 | 0.05 | 0.13 | 0.18 | 0.33 | 00.33 |
| Flash number | 11 | 12 | 13 | 14 | 15 | 16 | 17 | 18 | 19 | 20 |
| Date | 29.06.17 | 29.06.17 | 29.06.17 | 10.07.17 | 10.07.17 | 10.07.17 | 14.07.17 | 18.07.17 | 18.07.17 | 18.07.17 |
| UTC Time | 15:54:55 | 16:00:13 | 16:05:36 | 20:48:58 | 20:51:45 | 21:19:37 | 13:25:39 | 16:28:01 | 16:30:58 | 16:50:01 |
| Polarity | N | N | N | N | N | N | B | N | N | N |
| Type | ST | ST | ST | ST | ST | ST | ST | OT | OT | OT |
| LMA Active | 0.24 | 0.13 | 0.07 | 0.19 | 0.10 | 0.01 | 0.13 | 2.42 | 2.38 | 0.68 |

| | | | | | | | | | | |
|---|---|---|---|---|---|---|---|---|---|---|
| (%) | | | | | | | | | | |

## 5. Conclusions

We presented in this paper lightning current measurements and LMA data associated with upward flashes observed at the Säntis Tower during Summer 2017. The LMA network consisted of six stations located in the vicinity of the tower at distances ranging from 100 m to 11 km from it. We analyzed a total of 20 flashes that were simultaneously recorded by the current measurement system, fast electric field antenna and LMA in the period from 29.06.2017 to 18.07.2017.

Based on the EUCLID lightning activity in an area within 30 km from the tower and in a 5 s time window before the start of the flash only one of the 20 flashes was classified as OT. However, investigations based on the LMA data reveal that 3 more of the flashes were preceded by nearby activity. The results suggest that the number of OT flashes inferred from LLS data can be underestimated. The electric field measurements were available for three OT flashes and in all of them a preceding event can be observed.

We presented a detailed analysis of three OT flashes. The charge structure was inferred from the LMA measurements and the polarity of the leader from the horizontal speed of the leader and the current measurements at the tower. Simplified sketches for three OT flashes were presented.

The OT flashes occurred during two different storms. Both storms had predominantly positive lightning with a very shallow bottom negative charge layer or with an inverted charge structure. The LMA activity, measured by the number of located sources, was, on average, almost seven times higher compared to that during the ST flashes.

## 6. Acknowledgment

This work was supported in part by the Swiss National Science Foundation (Project No. 200020_175594), the European Union's Horizon 2020 research and innovation program under grant agreement No 737033-LLR, and the Spanish Ministry of Economy and the European Regional Development Fund (FEDER) ESP2015-69909-C5-5-R and ESP2017-86263-C4-2-R.

## 7. References

[1] Wang, D., Takagi, N., Watanabe, T., Sakurano, H., & Hashimoto, M. (2008). “Observed characteristics of upward leaders that are initiated from a windmill and its lightning protection tower”, Geophysical Research Letters, Vol. 35, 2008

[2] A. Smorgonskiy, A. Tajalli, F. Rachidi, M. Rubinstein and G. Diendorfer et al. An analysis of the initiation of upward flashes from tall towers with particular reference to Gaisberg and Säntis Towers, in Journal Of Atmospheric And Solar-Terrestrial Physics, vol. 136, p. 46-51, 2015.

[3] H. Zhou, G. Diendorfer, R. Thottappillil, H. Pichler, and M. Mair “The Influence of Meteorological Conditions on Upward Lightning Initiation at the Gaisberg Tower”, 2014 International Conference on Lightning Protection (ICLP), Shanghai, China

[4] A. Mostajabi et al., “On the Impact of Meteorological Conditions on the Initiation of Upward Lightning Flashes from Tall Structures,” in 2018 34th International Conference on Lightning Protection (ICLP), 2018.

[5] Heidler, F., M. Manhardt, and K. Stimper (2014), “Self-Initiated and Other-Triggered Positive Upward Lightning Measured at the Peissenberg Tower, Germany”, paper presented at the 2014 International Conference on Lightning Protection (ICLP),13–17 Oct, Shanghai

[6] T. Warner, K. Cummins and R. Orville, "Upward lightning observations from towers in Rapid City, South Dakota and comparison with National Lightning Detection Network data, 2004-2010", Journal of Geophysical Research: Atmospheres, vol. 117, no. 19, 2012.
[7] G.V.Cooray The Lightning Flash IEE, Power & Energy Series, 2003.
[8] C. Schumann , M. M.F. Saba, T. A. Warner, M. A. S Ferro "Upward Flashes Triggering Mechanisms", 2017 International Symposium on Lightning Protection (XIV SIPDA), Natal, Brazil, 2nd – 6th October 2017
[9] D. E. Proctor, "A hyperbolic system for obtaining VHF radio pictures of lightning," J. Geophys. Res., vol. 76, no. 6, pp. 1478–1489, Feb. 1971.
[10] D. E. Proctor, "VHF radio pictures of cloud flashes," J. Geophys. Res., vol. 86, no. C5, p. 4041, May 1981.
[11] D. E. Proctor, R. Uytenbogaardt, and B. M. Meredith, "VHF radio pictures of lightning flashes to ground," J. Geophys. Res., vol. 93, no. D10, p. 12683, Oct. 1988.
[12] B. R. Fuchs et al., "Environmental controls on storm intensity and charge structure in multiple regions of the continental United States," J. Geophys. Res. Atmos., vol. 120, no. 13, pp. 6575–6596, Jul. 2015.
[13] E. W. McCaul et al., "Forecasting Lightning Threat Using Cloud-Resolving Model Simulations," Weather Forecast., vol. 24, no. 3, pp. 709–729, Jun. 2009.
[14] D. R. MacGorman et al., "TELEX The Thunderstorm Electrification and Lightning Experiment," Bull. Am. Meteorol. Soc., vol. 89, no. 7, pp. 997–1013, Jul. 2008.
[15] W. Rison, R. J. Thomas, P. R. Krehbiel, T. Hamlin, and J. Harlin, "A GPS-based three-dimensional lightning mapping system: Initial observations in central New Mexico," Geophys. Res. Lett., vol. 26, no. 23, pp. 3573–3576, Dec. 1999.
[16] R. J. Thomas et al., "Accuracy of the Lightning Mapping Array," J. Geophys. Res., vol. 109, no. D14, p. D14207, Jul. 2004.
[17] A. Sunjerga et al., "On the Classification of Self-Triggered versus OtherTriggered Lightning Flashes," in 2018 34th International Conference on Lightning Protection (ICLP), 2018.
[18] C. Romero et al., "A system for the measurements of lightning currents at the Säntis Tower," Electr. Power Syst. Res., vol. 82, no. 1, pp. 34–43, 2012.
[19] C. Romero, F. Rachidi, M. Rubinstein, and M. Paolone, "Lightning currents measured on the Säntis Tower: A summary of the results obtained in 2010 and 2011," in 2013 IEEE International Symposium on Electromagnetic Compatibility, 2013, pp. 825–828.
[20] M. Azadifar, M. Paolone, D. Pavanello, F. Rachidi, C. Romero, and M. Rubinstein, "An Update on the Instrumentation of the Säntis Tower in Switzerland for Lightning Current Measurements and Obtained Results," in CIGRE Int. Colloquium on Lightning and Power Systems, 2014.
[21] C. Romero, F. Rachidi, M. Paolone, and S. Member, "Statistical Distributions of Lightning Currents Associated With Upward Negative Flashes Based on the Data Collected at the Säntis ( EMC ) Tower in 2010 and 2011," IEEE Trans. Power Deliv., vol. 28, no. 3, pp. 1804–1812, 2013.
[22] C. Romero, A. Mediano, A. Rubinstein, F. Rachidi, A. Rubinstein, and M. Paolone, "Measurement of Lightning Currents Using a Combination of Rogowski Coils and B-Dot Sensors," J. Light. Res., vol. 4, pp. 71–77, 2012.
[23] C. Romero, F. Rachidi, R. M., P. M., R. V. A., and D. Pavanello, "Positive Lightning Flashes Recorded on the Säntis Tower in 2010 and 2011," J. Geophys. Res., p. 12'879-12'892, 2013.
[24] D. Li et al., "On Lightning Electromagnetic Field Propagation Along an Irregular Terrain," IEEE Transactions on Electromagnetic Compatibility, vol. 58, no. 1, pp. 161–171, Feb. 2016.
[25] A. Mostajabi et al., "LMA Observation of Upward Flashes at Säntis Tower : Preliminary Results," in Joint IEEE International Symposium on Electromagnetic Compatibility & Asia-Pacific Symposium on Electromagnetic Compatibility, 2018, pp. 2–5
[26] W. Schulz, G. Diendorfer, S. Pedeboy, and D. R. Poelman, "The European lightning location system EUCLID – Part 1: Performance analysis and validation," Nat. Hazards Earth Syst. Sci, vol. 16, pp. 595–605, 2016
[27] W. Schulz, G. Diendorfer, S. Pedeboy, and D. R. Poelman, "The European lightning location system EUCLID – Part 1: Performance analysis and validation," Natural Hazards and Earth System Sciences, vol. 16, no. 2, pp. 595–605, Mar. 2016.

[28] J. T. Pilkey et al., “Rocket-triggered lightning propagation paths relative to preceding natural lightning activity and inferred cloud charge,” Journal of Geophysical Research: Atmospheres, vol. 119, no. 23, p. 13,427-13,456, Dec. 2014.
[29] O. A. van der Velde and J. Montanyà, “Asymmetries in bidirectional leader development of lightning flashes,” Journal of Geophysical Research: Atmospheres, vol. 118, no. 24, p. 13,504-13,519, Dec. 2013.
[30] H. W. Kasemir, “A contribution to the electrostatic theory of a lightning discharge,” Journal of Geophysical Research, vol. 65, no. 7, pp. 1873–1878, Jul. 1960.
[31] N. Pineda et al., “On the Meteorological Regimes Related to Upward Lightning at Säntis Tower (Switzerland), to be submitted to the Journal of Geophysical Research - Atmospheres